Journal of the European Ceramic Society 21 (2001) 1879–1882
www.elsevier.com/locate/jeurceramsoc

Characteristics of SnO_2-doped ZnO-based varistor ceramics

S. Bernik *, N. Daneu

Jožef Stefan Institute, Jamova 39, 1000 Ljubljana, Slovenia

Received 4 September 2000; received in revised form 11 October 2000; accepted 15 October 2000

Abstract

The Sb_2O_3 in a ZnO-based varistor composition was systematically substituted with SnO_2 in the range from 0 to 100%. The microstructural characteristics, average grain size and the general phase composition of the samples were not influenced by the substitutions. In all the samples we observed ZnO, Bi_2O_3-rich and spinel phase, where the composition of the spinel depends on the Sb_2O_3 to SnO_2 ratio in the starting composition. The non-linear coefficient α of the samples was not influenced by the SnO_2 substitution, while the threshold voltage decreases and the leakage current increased with larger additions of SnO_2. The capacitance–voltage measurements indicated strong increase in the donor density and the density of interface states at the grain boundaries while the depletion-layer width decreased and the barrier height was comparable in all the investigated samples. According to the electrical properties, SnO_2 had a strong donor effect in the ZnO varistor ceramics.

Keywords: Electrical properties; Microstructure-final; SnO_2 doping; Varistor; ZnO

1. Introduction

The exceptional non-linear current voltage (I–V) characteristics and energy-absorption capabilities of ZnO-based varistors are strongly related to their microstructure, which develops during the process of firing ZnO with small additions of Bi_2O_3, Sb_2O_3, Co_3O_4, Mn_3O_4, Cr_2O_3, NiO and other oxides. The current–voltage (I–V) non-linearity of the varistor is a grain-boundary phenomenon. A single non-ohmic grain boundary has a break-down voltage of 3 V. The number of non-ohmic grain boundaries between the electrodes determines the overall break-down voltage of the varistor and can be controlled either by varistor thickness or the ZnO grain size.[1] Sb_2O_3 is a standard additive in high-voltage ZnO-based varistor ceramics which require a fine-grained microstructure. The addition of Sb_2O_3 influences ZnO grain growth due to the formation of a $Zn_7Sb_2O_{12}$-type spinel phase and inversion boundaries in the ZnO grains.[2,3] The addition of SnO_2 to the ZnO-Bi_2O_3 system results in similar microstructural characteristics as observed for the addition of Sb_2O_3. SnO_2 reacts with ZnO to form a Zn_2SnO_4-type spinel phase and with Bi_2O_3 to form a $Bi_2Sn_2O_7$-type pyrochlore phase. It also triggers the formation of inversion boundaries in the ZnO grains.[4] Viswanath et al. reported that SnO_2 promotes the non-linear coefficient of the basic ZnO-Bi_2O_3 system.[5] However, very little research has been reported on the influence of SnO_2 on the characteristics of "real" ZnO-based varistor ceramics.

In the present work, we systematically substituted Sb_2O_3 with SnO_2 in "real" ZnO-based varistor compositions and observed the influence of SnO_2 on the microstructural properties, current–voltage (I–V) and capacitance–voltage (C–V) characteristics.

2. Experimental

Samples with nominal composition 96.2 mol% ZnO + 2.8 mol% ($Bi_2O_3 + Co_3O_4 + Mn_3O_4 + NiO + Cr_2O_3$) + ($1.0-x/2$) mol% Sb_2O_3 x mol% SnO_2 where $x = 0$, 0.2, 0.6, 1.0, 1.4 and 2.0 were prepared by the classical ceramic procedure. In these compositions, 0, 10, 30, 50, 70 and 100% of the Sb_2O_3 was substituted by SnO_2. The reagent-grade oxides were mixed in proper ratios and homogenised in absolute ethanol using a planetary mill. The powders were dried at 70°C and pressed with 200 MPa into discs with a diameter of 10 and 2 mm thickness. The pellets were fired in an alumina crucible at 1230°C

* Corresponding author. Tel.: +386-1-4773-682; fax: +386-1-4263-1126.

E-mail address: slavko.bernik@ijs.si (S. Bernik).

0955-2219/01/$ - see front matter
PII: S0955-2219(01)00135-2

for 2 h in an air atmosphere with heating and cooling rates of 5°C/min.

Densification characteristics were recorded using a heating-stage microscope (Leitz, Wetzlar) up to 1300°C at a heating rate of 10 K/min. The phase compositions of the samples were analysed by X-ray powder diffractometry (XRD; PW1710, Philips). The microstructures were examined using a scanning electron microscope (SEM; JSM-5800, Jeol) equipped with X-ray spectrometer (EDS; Link ISIS 300, Oxford Instruments). Cross-sections of the samples were mechanically ground and polished. The average ZnO grain sizes (D) of the samples were determined by measuring the surface of each ZnO grain and transforming its irregularly shaped area into a circle of equivalent diameter. For each sample 500–900 grains were taken into account.

For the DC current–voltage (I–V) characterisation, silver electrodes were painted on both surfaces of the discs and fired for 10 min at 590°C in air. The nominal varistor voltages (V_N) at 1 and 10 mA were measured for the purpose of determining the threshold voltage (V_T) and the non-linear coefficient (α). The leakage current (I_L) was measured at 0.75 V_N (1 mA). The C–V characteristics of the samples were measured at room temperature with an LCR meter (Hewlett Packard 4270 A) at a frequency of 10 kHz and a bias voltage in the 0–160 V range, controlled by a digital V-meter (Hewlett Packard 3456 A). According to the Schottky-barrier model and its C–V relation, the donor density (N_D), barrier height (Φ_B), density of interface states (N_S) and the depletion-layer width (t) were determined. N_D and Φ_B were determined from the slope and the intercept of the C–V line of the graph $(1/C_B - 1/2C_{B0})^2$ vs. V_G, and N_S and t were calculated from equations given elsewhere.[6,7,8]

3. Results and discussion

Microstructures of the sample doped only with SnO_2 and the sample doped only with Sb_2O_3 are presented in Fig. 1. It is clear that they are very similar. As the main phase, the samples contain ZnO grains with inversion boundaries and many intragranular spinel inclusions, while the Bi_2O_3-rich phase and spinel grains and are homogeneously distributed along the ZnO grain boundaries and multiple junctions. The average ZnO grain sizes of the samples with different Sb_2O_3 and SnO_2 ratios are between 11.1 and 12.5 μm (Table 1). Sintering curves of the samples with different amounts of both oxides (Fig. 2) show that the samples with higher SnO_2 additions start to densify at slightly lower temperatures, while sintering behaviour is similar for all investigated samples. These

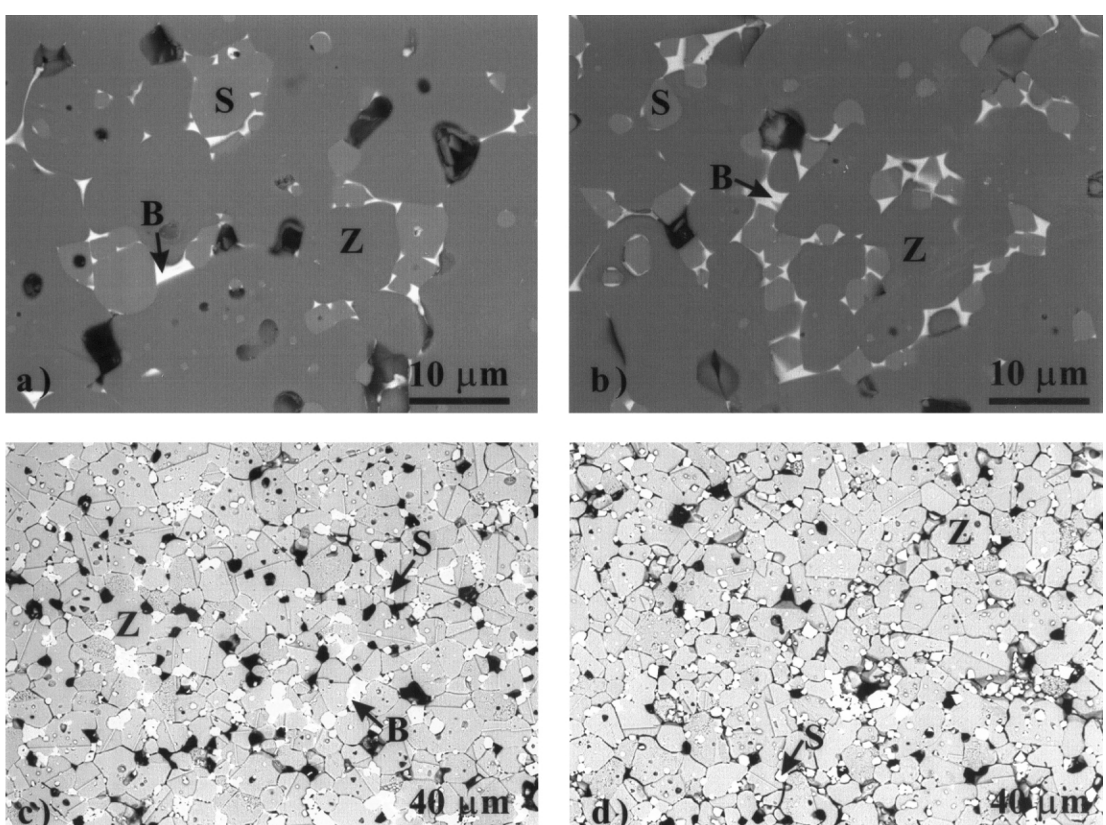

Fig. 1. Microstructures of ZnO-based varistor ceramics fired at 1230°C for 2 h: (a) unetched, with Sb_2O_3 only; (b) unetched, with SnO_2 only; (c) etched, with Sb_2O_3 only; and (d) etched, with SnO_2 only. Z: ZnO phase, B: Bi_2O_3-rich phase, S: spinel-type phase.

Table 1
The ZnO grain size (*D*) and I–V characteristics of the samples with different nominal compositions. (V_T — threshold voltage, α — non-linear coefficient, I_L — leakage current)

Sb_2O_3, substituted by SnO_2 (at. %)	*D* (μm)	V_T (V/mm)	α	I_L ($\times 10^{-3}$ A)
0	12.0	150	41	0.02
10	11.3	150	37	0.09
30	12.5	126	36	0.93
50	11.6	129	44	0.93
70	12.0	131	46	1.58
100	11.1	127	43	8.20

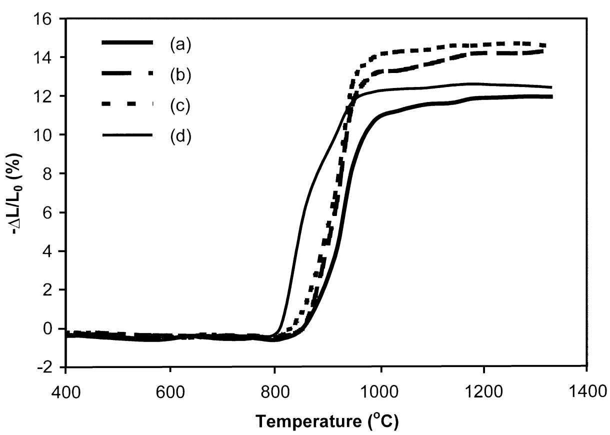

Fig. 2. Densification curves of ZnO-based varistor samples with the addition of SnO_2 and Sb_2O_3 in different atomic ratios: (a) 0% SnO_2 + 100% Sb_2O_3, (b) 30% SnO_2 + 70% Sb_2O_3; (c) 70% SnO_2 + 30% Sb_2O_3; and (d) 100% SnO_2 + 0% Sb_2O_3.

general microstructural observations indicate that Sb_2O_3 and SnO_2 have very similar effects on the microstructure development of the investigated varistor composition. EDS analysis of secondary phases showed that in the samples which contain only Sb_2O_3 or SnO_2 the corresponding Zn_2SnO_4- and $Zn_7Sb_2O_{12}$-type spinel phases form, containing dissolved Cr, Mn, Ni and Co. In the samples with different additions of both oxides, Sb_2O_3 and SnO_2, the spinel phase contains cations from both oxides in an Sb/Sn atomic ratio corresponding to the Sb_2O_3/SnO_2 ratio of the nominal composition of these samples. The size and morphology of the spinel grains are similar in all samples. Mostly they are intergranular, however they can also be frequently observed as inclusions in ZnO grains, sometimes caught up together with some Bi_2O_3-rich phase. In the samples with 50 and 70% SnO_2 additions, traces of pyrochlore phase were observed. Similar to the observations of the spinel phase, it also has a mixed composition, containing both Sn and Sb cations along with some dissolved Cr, Mn, Co and Ni. In the ZnO–Bi_2O_3–Sb_2O_3 system, the $Bi_3Zn_2Sb_3O_{11}$-type pyrochlore phase forms below 700°C, then it decomposes to the $Zn_7Sb_2O_{12}$ spinel and Bi_2O_3 liquid phase above 1000°C and on slow cooling it forms reversibly from the decomposition products.[9] Our previous results showed similar behaviour for the $Bi_2Sn_2O_7$-type pyrochlore phase.[4] However, it is well known that the presence of Cr_2O_3 can prevent reformation of the $Bi_3Zn_2Sb_3O_{11}$ pyrochlore on cooling.[9] The results from this study indicate that the addition of Cr_2O_3 may also prevent the reformation of the $Bi_2Sn_2O_7$-type pyrochlore on slow cooling since no pyrochlore was observed in most samples with additions of SnO_2.

The results of XRD analyses (Fig. 3) show that the stable modification of the Bi_2O_3-rich phase in the sample with the addition of Sb_2O_3 only is γ-Bi_2O_3 while with higher additions of SnO_2 the stable modification is β-Bi_2O_3. The XRD analysis of the samples after firing with electrodes at 590°C showed the presence of the γ-Bi_2O_3 phase in all the investigated samples. The diffraction patterns also agree with the results of our EDS analyses of the spinel phase which showed a mixed composition of the spinel phase in the samples with different Sb/Sn ratios. The Zn_2SnO_4 spinel has a slightly larger unit cell than $Zn_7Sb_2O_{12}$, therefore, the characteristic peaks of the spinel phases shift to higher *d*-values with increasing additions of SnO_2.

The results of the current-voltage (I–V) characterisation of the samples are given in Table 1. The non-linear coefficient α is around 40 for all samples and is not significantly affected by the SnO_2 addition. On the other hand, we observed a significant increase in the leakage current (I_L) and a decrease of the threshold voltage (V_T) with larger additions of SnO_2. The capacitance-voltage (C–V) characteristics of the samples (Fig. 4) and the characteristic C–V parameters, determined from these characteristics (Table 2), indicate that the substitution of Sb_2O_3 with SnO_2 results in a significant increase in the donor density (N_D) and the density of interface states (N_S), while the barrier height (Φ_B) is comparable in all the samples and is around 1.15±0.5 eV. The depletion-layer width (t) decreases from 30 to 15 nm with increasing amounts of SnO_2. The measurements of

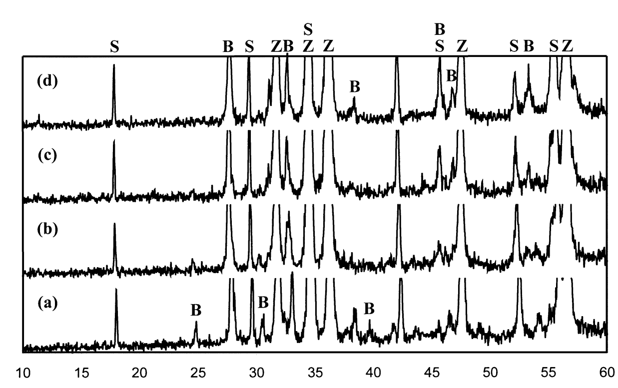

Fig. 3. XRD patterns of investigated samples with additions of SnO_2 and Sb_2O_3 in different atomic ratios: (a) 0% SnO_2 + 100% Sb_2O_3; (b) 30% SnO_2 + 70% Sb_2O_3; (c) 70% SnO_2 + 30% Sb_2O_3; and (d) 100% SnO_2 + 0% Sb_2O_3; Z:ZnO, B: Bi_2O_3 phase, S: spinel phase.

Table 2
Characteristic C–V parameters of the investigated samples. (N_D — donor density, N_S — density of interface states, Φ_B — the barrier height, t - width of the depletion layer)

Sb_2O_3 substituted by SnO_2 (at. %)	N_D ($\times 10^{18}$ cm^{-3})	N_S ($\times 10^{12}$ cm^{-2})	Φ_B (eV)	t (nm)
0	1.47	4.00	1.17	28
10	1.12	3.55	1.20	32
30	1.96	4.50	1.10	23
50	4.18	6.49	1.12	17
70	4.61	7.07	1.17	16
100	5.84	7.84	1.15	14

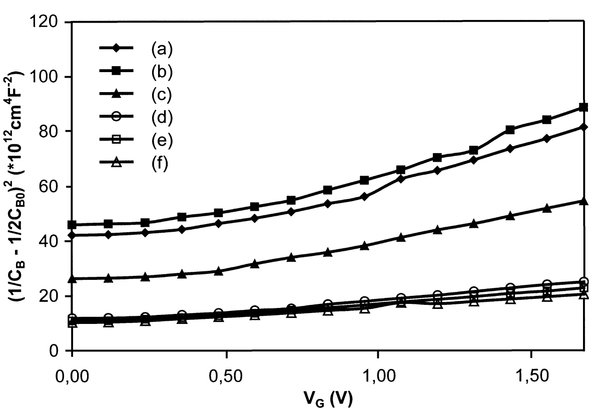

Fig. 4. The C–V characteristics of ZnO-based varistor samples with Sb_2O_3 substituted by SnO_2 in different atomic ratios: (a) 0% SnO_2 + 100% Sb_2O_3; (b) 30% SnO_2 + 70% Sb_2O_3; (c) 50% Sb_2O_3 + 50% SnO_2; (d) 70% SnO_2 + 30% Sb_2O_3; and (e) 100% SnO_2 + 0% Sb_2O_3; C_B: capacitance per unit area of grain boundary, C_{B0}: value of C_B when $V_G = 0$, V_G: applied voltage per grain boundary.

the electrical properties of the samples with the substitution of Sb_2O_3 by SnO_2 indicate that SnO_2 has a strong donor effect which contributes to the increase of the leakage current (I_L) in the samples with higher amounts of SnO_2.

4. Summary

Sintering of ZnO doped with Bi_2O_3, Co_3O_4, Mn_2O_3, NiO, Cr_2O_3 and different additions of Sb_2O_3 and SnO_2 at 1230°C for 2 h results in similar microstructures with average grain sizes from 11.1 to 12.5 μm. In the samples with the addition of both SnO_2 and Sb_2O_3 a mixed spinel phase forms which contains cations from both oxides in an Sb/Sn atomic ratio corresponding to the Sb_2O_3/SnO_2 ratio in the nominal composition of these samples.

The non-linear coefficient α is not affected by the substitution of Sb_2O_3 with SnO_2 and ranges from 36 to 46. In the samples with larger SnO_2 additions the leakage current increases from 0.02 to 8.2×10^{-3}A and the threshold voltage decreases from 150 to 127 V/mm. The capacitance-voltage measurements showed that in the samples with larger additions of SnO_2 the donor density at the grain boundaries increases from 1.47 to 5.84×10^{18} cm^{-3}, the depletion-layer width decreases from 28 to 14 nm, while the barrier height is approximately 1.15eV for all samples.

Our results show that substitution of Sb_2O_3 with SnO_2 does not influence the general microstructural characteristics, but the addition of SnO_2 has a strong donor effect in the ZnO-based varistor ceramics, which results in a significant increment of the leakage current.

Acknowledgements

The financial support of the Ministry of Science and Technology of Slovenia is gratefully acknowledged.

References

1. Gupta, T. K., Application of zinc oxide varistors. *J. Am. Ceram. Soc.*, 1990, **73**(7), 1817–1840.
2. Asokan, T., Iyengar, G. H. K. and Nagabhushana, G. R., Studies on microstructure and density of sintered ZnO-based non-linear resistors. *J. Mater. Sci.*, 1987, **22**(6), 2229–2236.
3. Senda, T. and Bradt, R. C., Grain growth of zinc oxide during the sintering of zinc oxide–antimony oxide ceramics. *J. Am. Ceram. Soc.*, 1991, **74**(6), 1296–1302.
4. Daneu, N., Recnik, A., Bernik, S. and Kolar, D., Microstructure development in SnO_2-doped ZnO–Bi_2O_3 ceramics. *J. Am. Ceram. Soc.*, 2000, **83**(12), 3165–3171.
5. Viswanath, R. N., Ravi, P. and Ramasamy, S., Preparation and characterisation of ZnO based materials for varistor applications. *Trans. Indian Inst. Met.*, 1995, **48**(3), 221–224.
6. Mukae, K., Tsuda, K. and Nagasawa, I., Capacitance-vs-voltage characteristics of ZnO varistors. *J. Appl. Phys.*, 1979, **50**(6), 4475–4476.
7. Fan, J. and Freer, R., The electrical properties and d.c. degradation characteristics of silver doped ZnO varistors. *J. Mater. Sci.*, 1993, **28**, 1391–1395.
8. Sun, H. T., Zhang, L. Y. and Yao, X., Electrical nonuniformity of grain boundaries within ZnO varistors. *J. Am. Ceram. Soc.*, 1993, **76**(5), 1150–1155.
9. Cho, S. G., Lee, H. and Kim, H. S., Effect of chromium on the phase evolution and microstructure of ZnO doped with bismuth and antimony. *J. Mater. Sci.*, 1997, **32**(16), 4283–4287.